Low-Frequency Modes of Atmospheric Variability Affecting the Formation of Meteorological Conditions over Northern Eurasia in Summer

Kulikova I.A., Kruglova E.N., Kryjov V.N.
HYDROMETETEOROLOGICAL RESEARCH CENTRE OF RUSSIAN FEDERATION, MOSCOW

Regional Climate Outlook Forum (NEACOF-16)

Moscow, 3 June, 2019

TABLE OF CONTENTS

Part I: The background information

1. Introduction: long-range forecast objects
2. Physical assumptions
3. Definitions of low frequency variability
4. Research methods

Part II: Low-Frequency Modes of Atmospheric Variability

1. Teleconnection patterns
2. Hydrodynamic forecasts
3. Diagnostic verification
4. Operational work
5. Extreme events

Summary

INTRODUCTION

Long-range forecasts is occupied a special place in the activity of world meteorological centers. A hydrodynamic theory of large-scale atmospheric processes involve complex issues, one of which is the issue of predictability. According to the limit of predictability, we can talk only about getting as much useful information about the statistical characteristics of meteorological conditions for each season and geographical region. Hardly ever made people a chance to answer the question: "Will be a rain in the given place at the given day of next month or season?"
The task of long-range forecasts is reduced to the definition of

global circulation anomalies (El Niño - Southern Oscillation - ENSO , monsoons, planetary waves),

averaged over a given time interval (month, season) meteorological fields or weather characteristics (mainly temperature and precipitation),

probability of three equiprobable categories for main meteorological characteristics.

PHYSICAL ASSUMPTIONS

The practical predictability interval is 5-7 day. It may be increased up to 2 – 3 weeks depending on a season, region and stability of atmospheric circulation.

The first kind of predictability is, firstly, restricted by sensitvity to uncertainty of initial conditions, and, secondly, by branching because of bifurcation in nonlinear systems. Even small disturbances (similar to a wave of wings butterflies) can change results of integration of General Circulation Models (GCM).

Predictability of the second kind, in which the object is to predict the evolution of the statistical properties of the system in response to changes in external forcings over time. Predictability of the second kind is essentially a boundary value problem, requiring good information on all boundary conditions which might influence system over time, e.g., variations of sea surface temperature, a surface of a land (an ice, a snow cover and humidity of ground). These parameters are more inertial that is why it is easier to predict environments. The other important external conditions are luminosity of the Sun, a content of hotbed gases, volcanic eruption, etc.. The predictability of the second kind defines possibilities of the forecast of large-scale structures of atmospheric circulation, as well as statistical characteristics of meteorological fields on seasonal and longer intervals of time.

DEFINITIONS

At present, it is conventionally assumed that the low frequency range in the general circulation of the atmosphere covers oscillations outside the synoptic variability.

- Variability with characteristic time scales of more than 10 days (Dymnikov V.P.).
- Atmospheric fluctuations with time scales of the order of a week or more (J. Wallace J., Blackmon M.).
- Multanovsky introduced the concept of "natural synoptic period", which was defined as such a period of time during which a process oriented in a certain way develops while retaining the "sign of the pressure field" in the space of the "natural synoptic region". This period covers about 6 - 8, an average of 7 days.

RESEARCH METHODS

- Dynamic stochastic approach;
- Spectral methods (variability as a function of frequency and zonal wave number);
- Correlation analysis. The most widely used in practice are the "teleconnections" of Wallace and Gutzler, 1981, chosen on the basis of considering temporal correlation coefficients at all possible pairs of grid points (monthly mean sea level pressure and 500 mb height analyses).
- Factor analysis, analysis of long-term circulation anomalies (Lau 1981; Dole 1983), rotated empirical orthogonal functions (Horn, 1981; Barnston and Livezey 1987; Richman 1986), EOF, "types of main oscillations" (Principal Oscillation Patterns, POPs) and "types of main oscillations over limited time" (Finite-Time Principal Oscillation Patterns, FTPOPs) (Frederiksen and Branstator 2005).
- Synoptic methods.

DYNAMIC STOCHASTIC APPROACH

- 0-hypothesis - low-frequency variability is explained by the response of circulation to the stochastic effect of high-frequency vortices. Low-frequency variability is simply red noise, the formation of which can be described by a linear dynamic-stochastic equation:

$$\frac{d\varphi}{dt} + A\varphi = f$$

where f – δ is a time-correlated random process. Operator A can be understood in the first approximation as an operator obtained by linearizing barotropic equations with respect to a zone-asymmetric flow.
The main conclusion: most of the low-frequency variability of the atmospheric circulation can be explained using the linear dynamic-stochastic model.

Dymnikov V.P. Stability and predictability of large-scale atmospheric processes. M, 2007.

SPECTRAL ANALYSIS

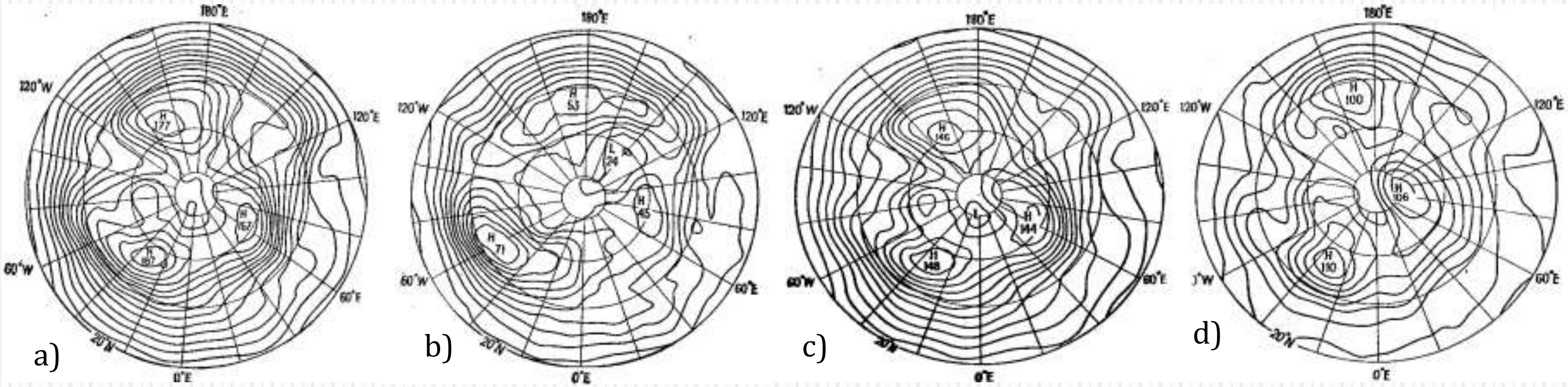

Maps of the variability (root-mean-square) of the 500 mb geopotential height for Northern Hemisphere (a 18-year record, 1962/63 to 1979/80, winter is a 90-day period starting on 1 `December): (a) all waves - unfiltered data, contour interval 10 m; (b) a data filtered by a high-frequency filter that transmits oscillations with periods of 2.5 to 6 days, contour interval 5 m); (c) a data filtered by a low-pass filter that transmits vibrations with periods longer than 10 days, contour interval 5 m; d) a data filtered by a low-pass filter that transmits vibrations with 30-day periods, contour interval 10 m.

Дж. Уоллес, М. Блэкмон. Наблюдаемая низкочастотная изменчивость в атмосфере. В кн. // Крупномасштабные динамические процессы в атмосфере, М.: Мир, 1988, стр. 66-109.

TELECONNECTION PATTERNS

$$I_{PNA} = \frac{1}{4}\left[z(A) - z(B) + z(C) - z(D)\right]$$

$$I_{WA} = \frac{1}{2}\left[z(N) - z(I)\right]$$

$$I_{EA} = \frac{1}{4}\left[2z(F) - z(E) - z(G)\right]$$

$$I_{EU} = \frac{1}{4}\left[-z(L) + 2z(M) - z(H)\right]$$

$$I_{WP} = \frac{1}{2}\left[z(J) - z(K)\right]$$

z – normalized 500 mb height anomalies

The most reproducible of this patterns are what we have referred to as Pacific/North American pattern (PNA) which has been previously noted by Namias and collaborators, and Western Atlantic pattern (WA), which is closely related so-called North Atlantic Oscillation identified by Walker and Bliss (1932). The other patterns are East Atlantic (EA), West Pacific (WP,), Eurasian (EU).

The authors make use of monthly mean sea level pressure and 500 mb height data for 45 months (Decembers, Januarys, and Februarys for 15 winters 1962-63 through 1976-77). They consider one-point correlation maps for the some centers of maximum teleconnectivity. The leading eigenvectors of the correlation matrix are used too. Patterns of a more regional scale, more clearly defined at mid-tropospheric levels than at the earthe's surface.

Wallace J.M. and Gutzler D.S. Teleconnection in geopotential height field during the Northern Hemisphere winter.- Mon. Wea. Rev., 1981, vol.109, pp. 784-812.

FACTOR ANALYSIS

Consider the scalar function F (t, x) describing a certain set of fields given at fixed times t_j, j=1,...,n, over certain area of the numbered points x_i, i=1,…m. According to the classical factor analysis model, the following decomposition takes place:

$$F(t_j, x_i) = \sum_{r=1}^{k} A_r(x_i) G_r(t_j) + \sum_{q=1}^{m} D_q(x_i) E_q(t_j)$$

where A_r (x_i) and D_q(x_i) loads respectively with common A_r (x_i) and specific factors D_q(x_i).

We used a data set consisting of
Daily (for 0 hours of the Greenwich Mean Time) fields of the 500 mb height for 1967-1987, at 212 points over of the Northern Hemisphere from 20N to 90N. The analysis was carried out separately for each of 12 calendar months.

Kulikova I.A., Resnyansky Yu.D. Low-frequency variability and types of atmospheric circulation, Meteorology and Hydrology, 1995, No. 10, p. 5-12.

TELECONNECTION PATTERNS

ARCTIC OSCILLATION

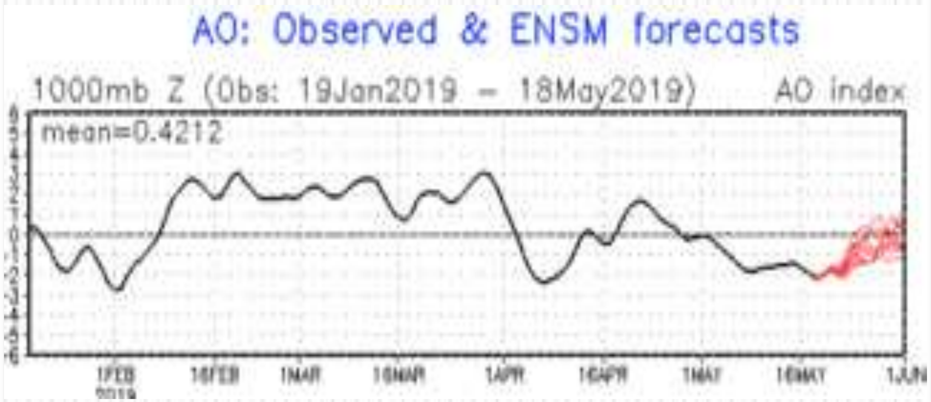

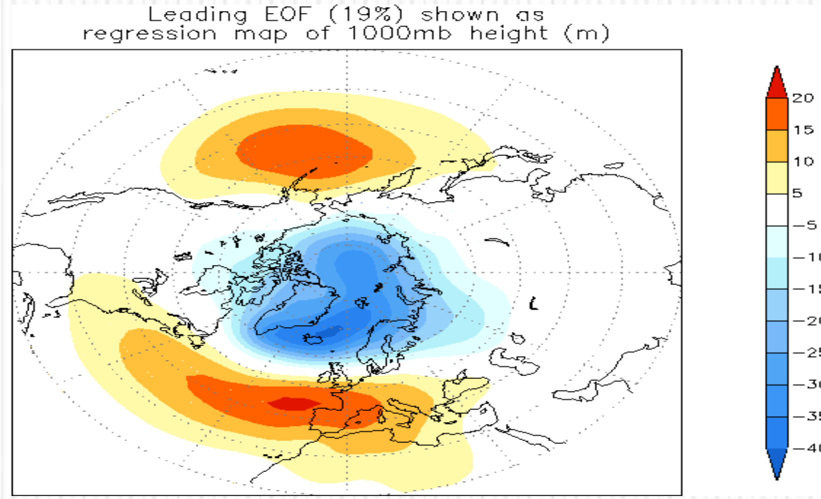

NORTH-ATLANTIC OSCILLATION

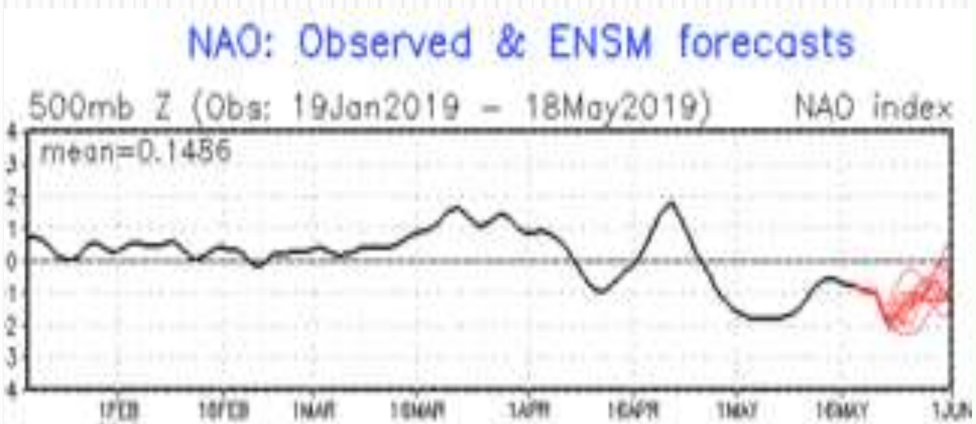

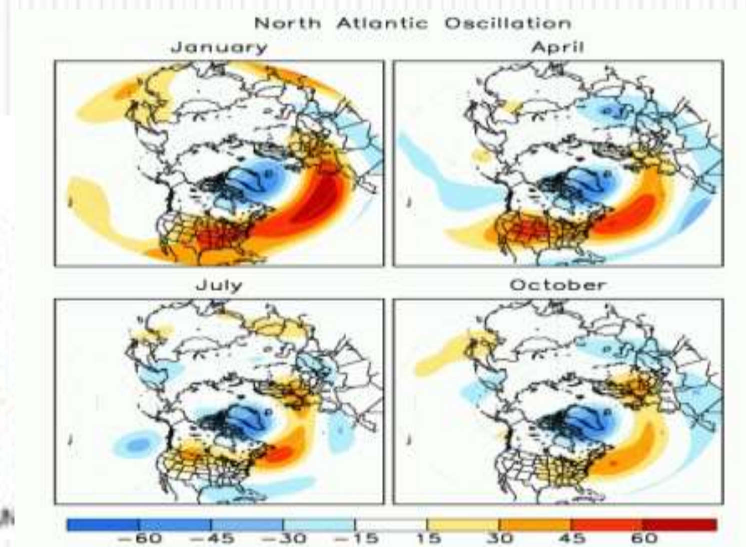

Barnston and Livezey 1987,
http://www.cpc.ncep.noaa.gov/products/precip/CWlink/daily_ao_index/teleconnections.shtml

TELECONNECTION PATTERNS

EA	East Anlantic	Wallace J. M., Gutzler D.S. Teleconnections in the geopotential height field during the Northern Hemisphere winter. – Mon. Wea. Rev., 1981, vol. 109, pp. 784-812
WA	West Anlantic	
EU	Eurasian	
WP	West Pacific	
PNA	Pacific-North American	
NAO	North-Atlantic oscillation	Climate Prediction Centre of USA, http://www.cpc.ncep.noaa.gov/
POL	Polar oscillation	
AOS	Arctic oscillation	

Quartile Analysis of Indices

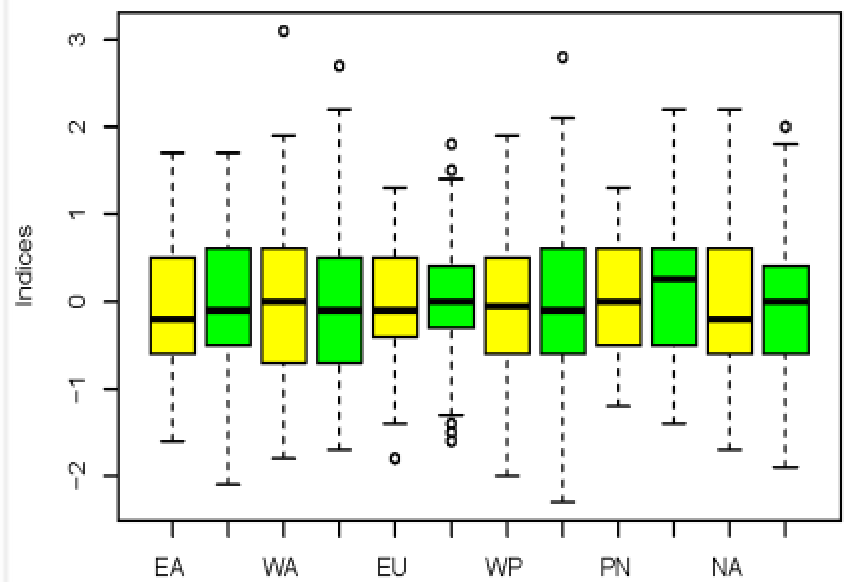

Index	Q1 (25%)	Q3 (75%)
EA	-0.493	0.485
WA	-0.559	0.494
EU	-0.452	0.458
WP	-0.544	0.501
PNA	-0.386	0.404
NAO	**-0.487**	**0.632**
POL	**-0.487**	**0.632**
AOS	**-0.884**	**0.87**

The indices were further partitioned by the help of 25% and 75% quartiles. These levels were taken as boundary values, which allow identifying the positive, neutral, and negative phases of each index and the associated atmospheric circulation regimes.

COMPOSITE MAPS

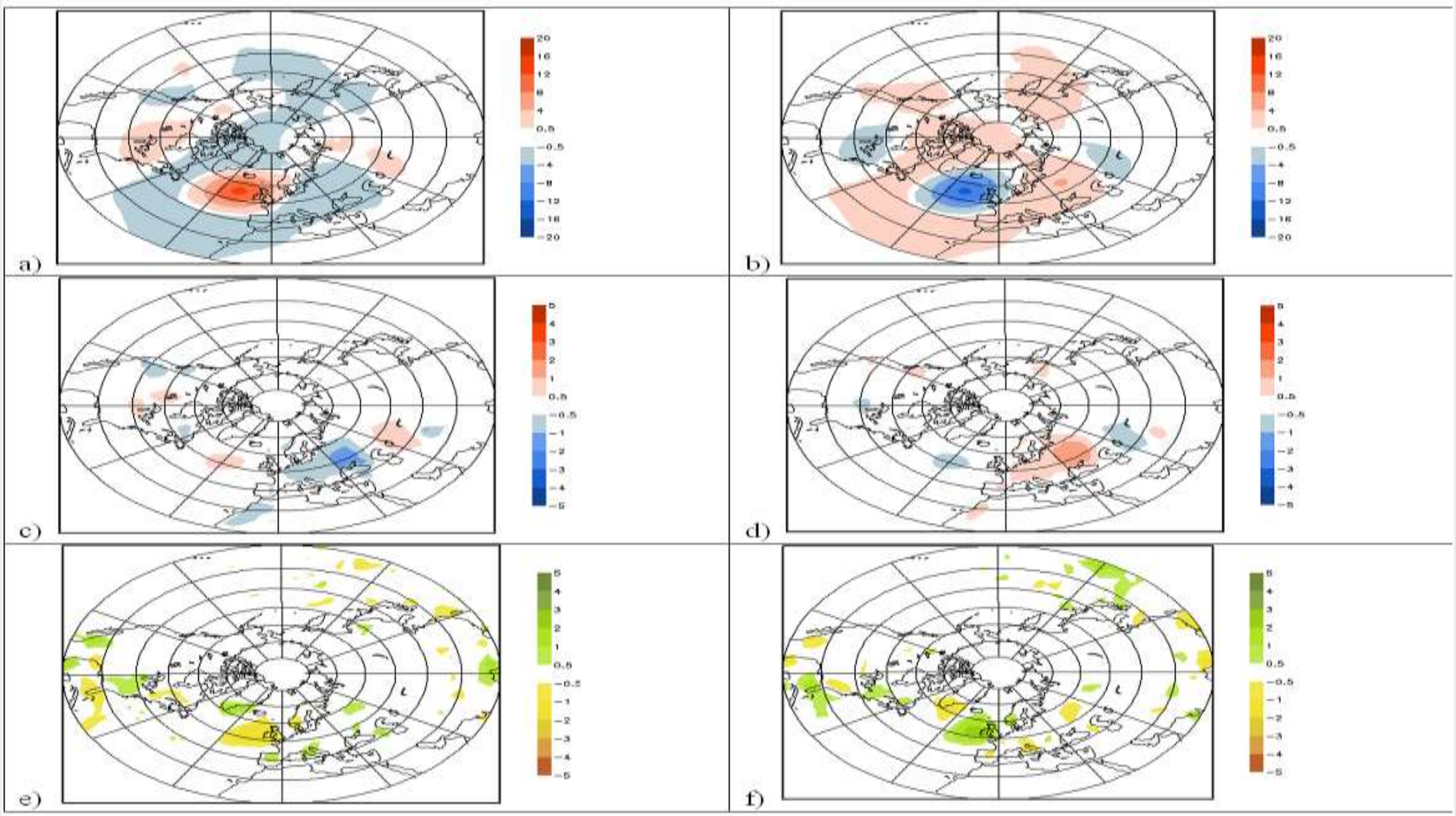

Summer. Composite maps constructed for a) H-500 fields (dam), b) surface air temperature (° C) and c) precipitation (mm / day) in the case of the positive phase of the EA index> 0.48; d)H-500 fields (dam), e) surface air temperature (˚C) and f) precipitation (mm / day) in case of a negative phase of the EA <-0.49 index.

COMPOSITE MAPS

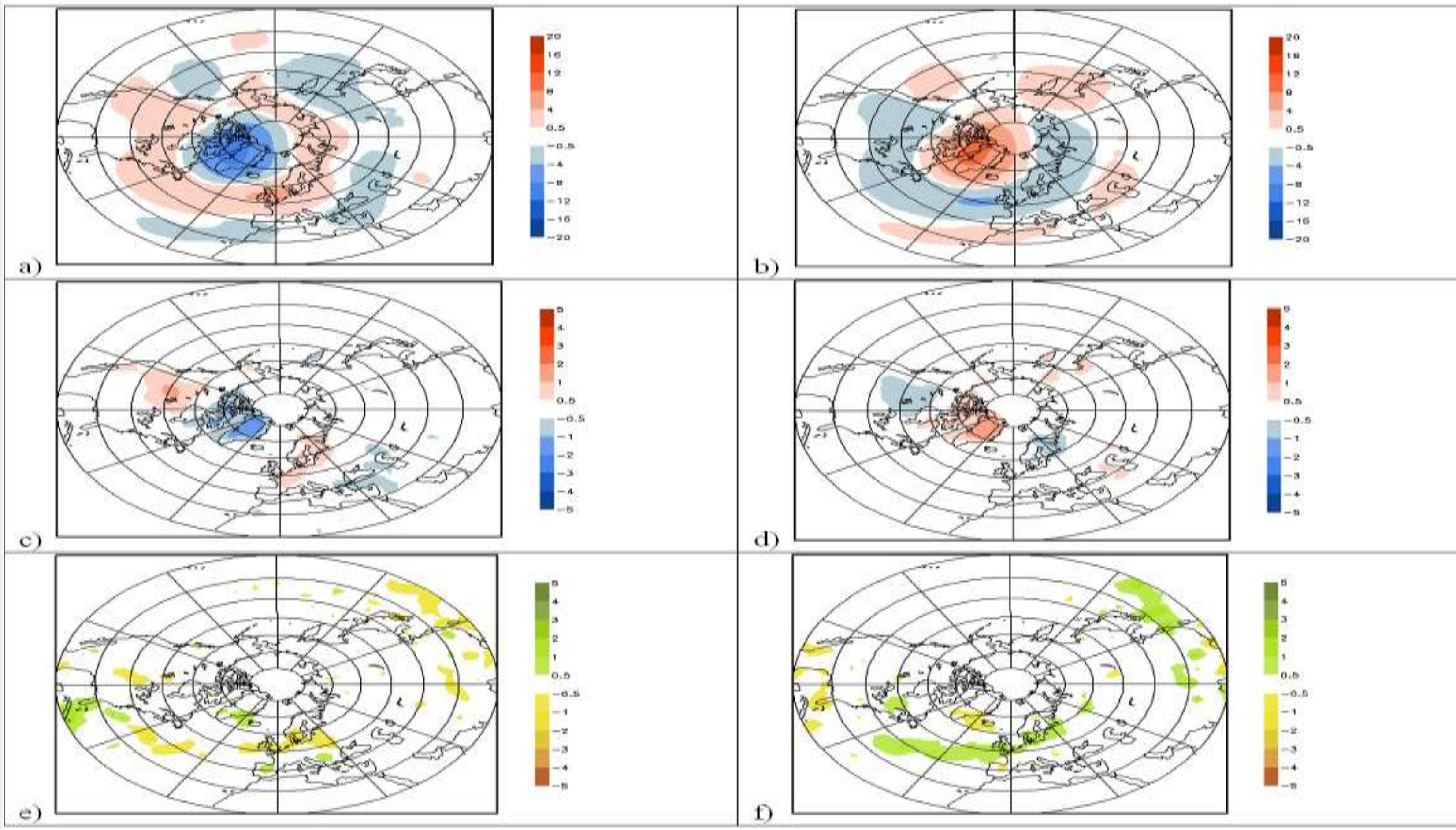

Summer. Composite maps constructed for a) H-500 fields (dam), b) surface air temperature (° C) and c) precipitation (mm / day) in the case of the positive phase of the NAO index> 0.63; d)H-500 fields (dam), e) surface air temperature (˚C) and f) precipitation (mm / day) in case of a negative phase of the NAO <-0.49 index.

COMPOSITE MAPS

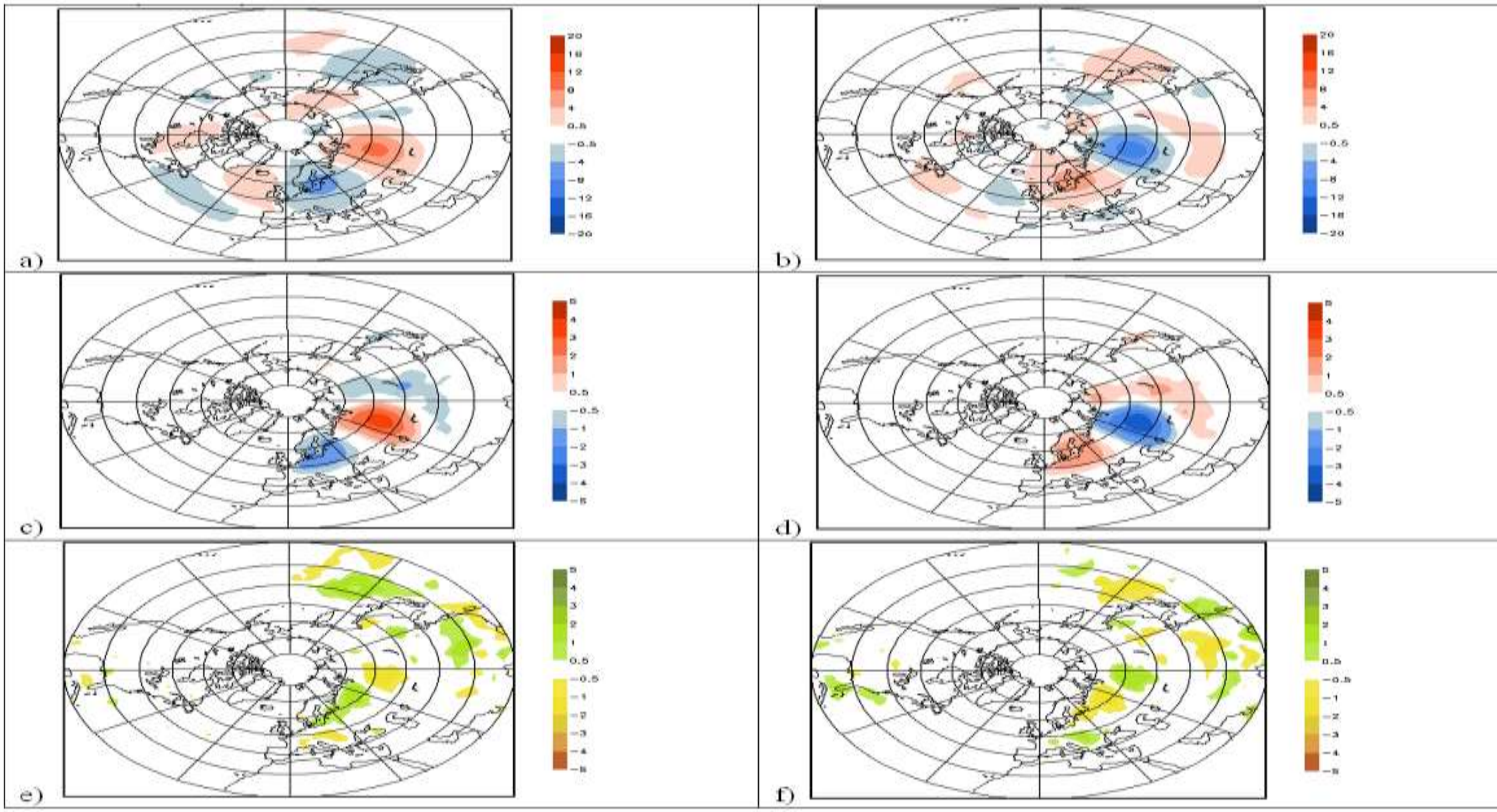

Summer. Composite maps constructed for a) H-500 fields (dam), b) surface air temperature (° C) and c) precipitation (mm / day) in the case of the positive phase of the EU index> 0.46; d)H-500 fields (dam), e) surface air temperature (˚C) and f) precipitation (mm / day) in case of a negative phase of the EU <-0.45 index.

COMPOSITE MAPS

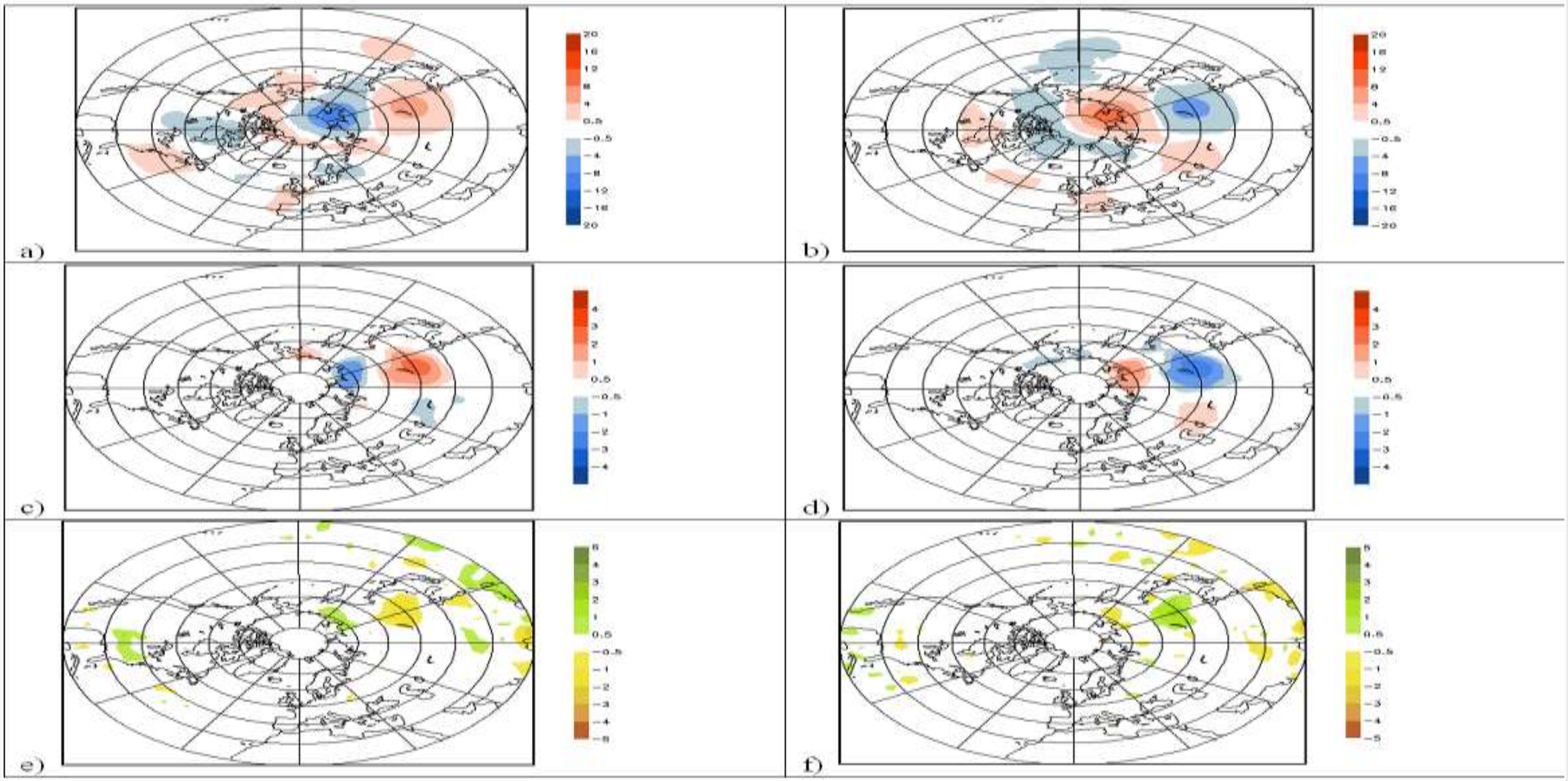

Summer. Composite maps constructed for a) H-500 fields (dam), b) surface air temperature (° C) and c) precipitation (mm / day) in the case of the positive phase of the POL index> 0.53; d)H-500 fields (dam), e) surface air temperature (˚C) and f) precipitation (mm / day) in case of a negative phase of the POL <-0.52 index.

COMPOSITE MAPS

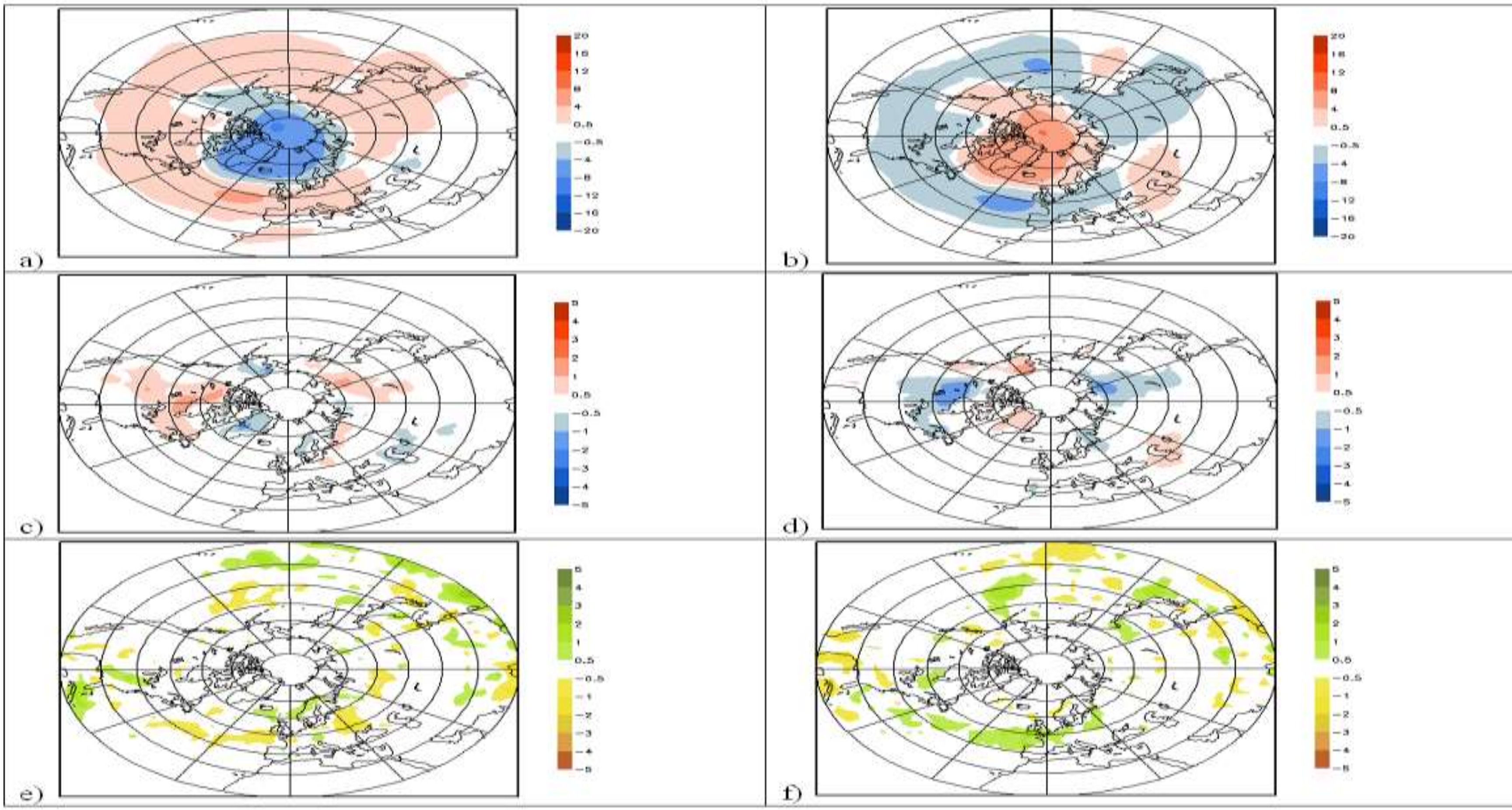

Summer. Composite maps constructed for a) H-500 fields (dam), b) surface air temperature (° C) and c) precipitation (mm / day) in the case of the positive phase of the AO index> 0.87; d)H-500 fields (dam), e) surface air temperature (˚C) and f) precipitation (mm / day) in case of a negative phase of the AO <-0.88 index.

HYDRODYNAMIC FORECASTS

- The hindcasts of 500 mb (H-500) height fields for the period from 1981 to 2010, based on the global semi-Lagrangian model (SL-AV) developing at the HMC of Russia are used. The model has a spatial resolution of 1.125º latitude and 1.40625º longitude and 28 vertical levels. It generates 10 members of the ensemble based on the initial reanalysis-2 NCEP / NCAR using the breeding method. The boundary conditions are the initial anomalies of sea surface temperature (SST) during the entire prognostic period. A detailed description of the model is given in [M. Tolstykh et al.]. In this study, we make use of only deterministic forecasts (mean ensemble) of the mean monthly 500 mb (H-500) height fields (on 1-4 month lead forecast) and seasonal (on 1–3 and 2-4 season lead forecast).
- It is of interest to compare the results of hydrodynamic modeling with the mean monthly 500 mb (H-500) height fields (reanalysis), obtained on the basis of the NCEP / NCAR archive on a 2.5°x2.5.

HYDRODYNAMIC FORECASTS

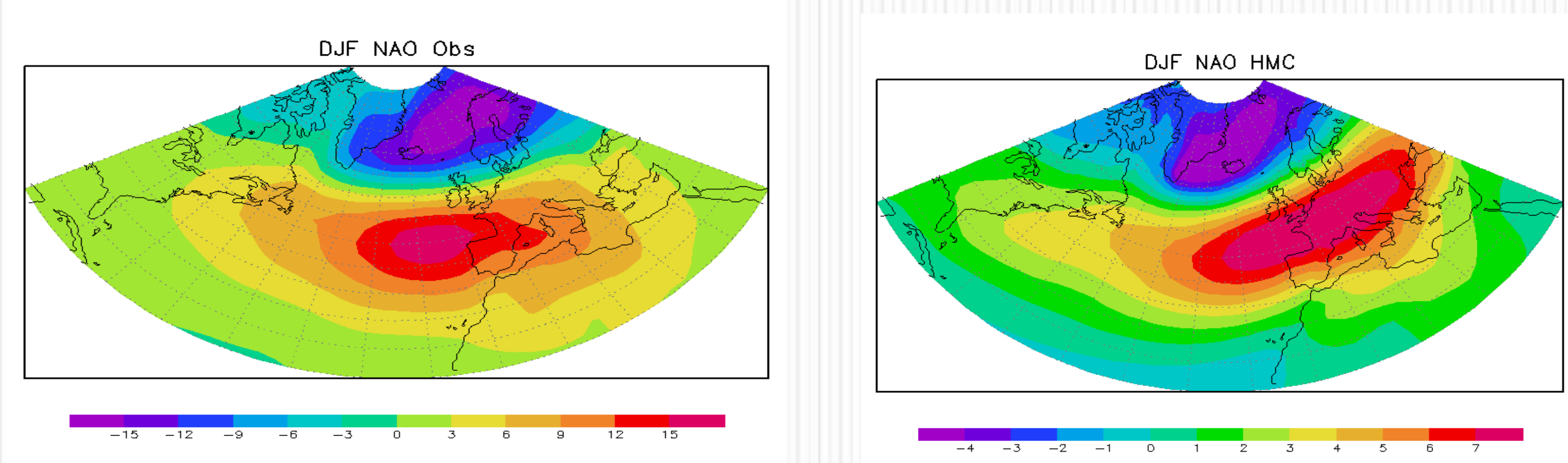

The first empirical orthogonal function of the sea level pressure from observational data (left) and hydrodynamic modeling (right) (Kryzhov V.N.)

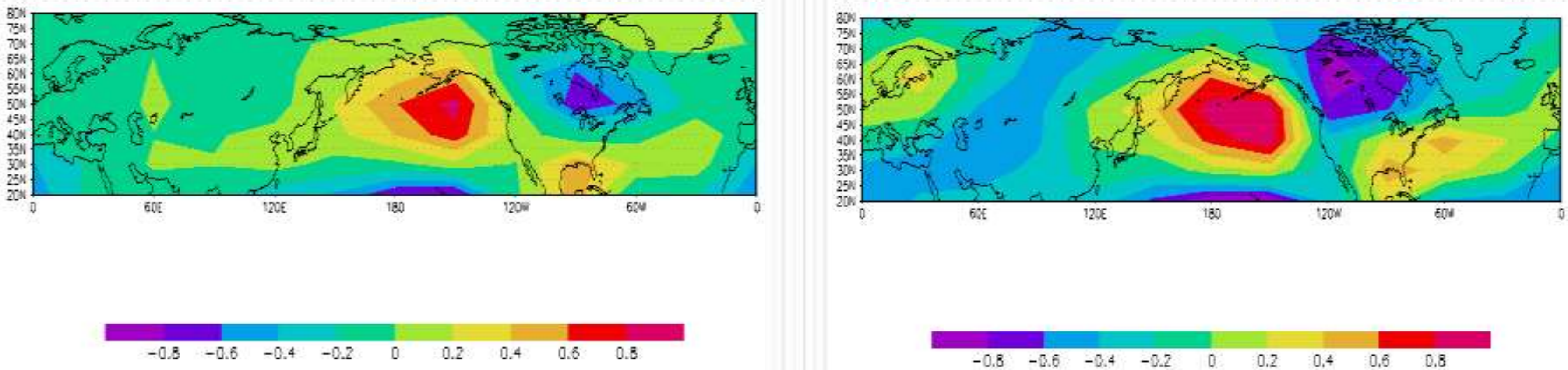

Factor loads after an oblique rotation of loading matrix: factor 3 computed from reanalysis (left) and factor 4 computed from hindcasts (right) for the winter period.

DIAGNOSTIC VERIFICATION

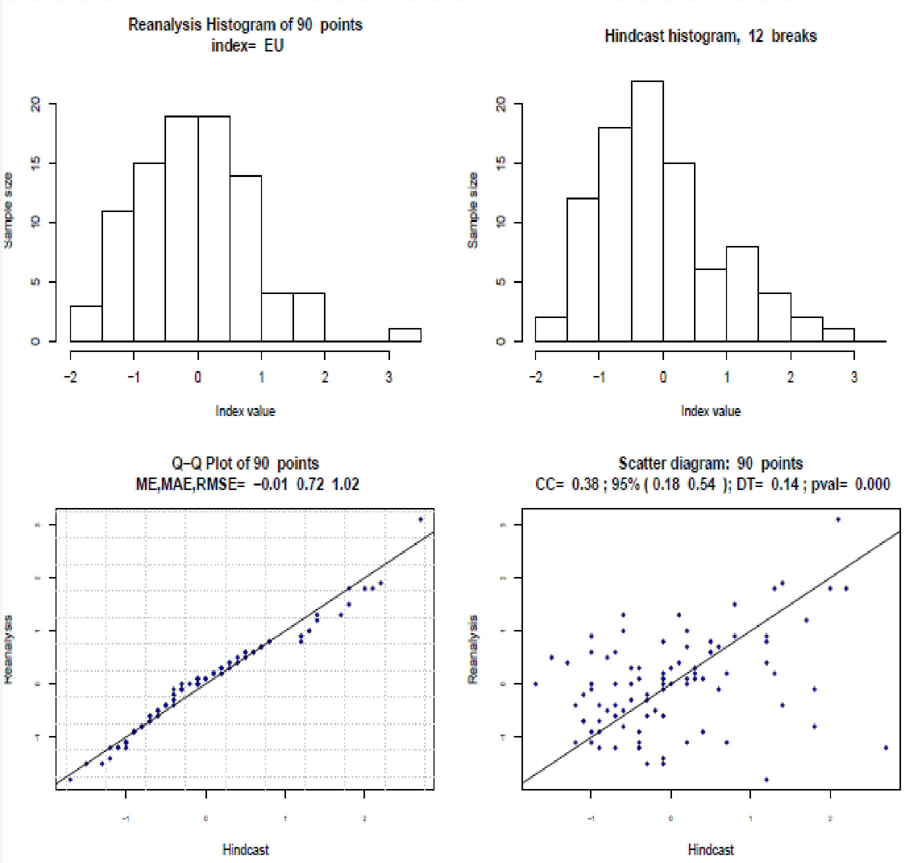

Diagnostics of hindcasts of monthly mean Eurasian Oscillation Index (EU) on 1 month lead forecast for the summer period: a) histogram of reanalysis; b) histogram of hindcasts; c) quantile diagrams; d) scatterplot.

Kiktev D.B., Kruglova E.N..Kulikova I.A, Low-Frequency Modes and Atmospheric Variability: Part I. Statistical analysis and hydrodynamic simulation. Met. and Hyd., 2015, no 3, p. 5-22.

Kulikova I.A, Kruglova E.N.. , Kiktev D.B. Low-Frequency Modes and Atmospheric Variability: Part II. The impact of modes on the temperature and precipitation spatial distribution in the North Eurasia. Met. and Hyd., 2015, no 4, p. 5-16.

VERIFICATION

Index	ME	MAE	RMSE	CC	CC1	CC2	DT	pval
				summer, 1 -month				
EA	0.00	0.55	0.69	0.46	0.28	0.61	0.21	0.00
EU	0.00	0.56	0.74	0.46	0.28	0.62	0.21	0.00
NAO	0.00	0.62	0.81	0.23	0.02	0.42	0.05	0.03
PNA	0.00	0.53	0.66	0.44	0.26	0.60	0.20	0.00
WA	0.00	0.68	0.84	0.24	-0.03	0.42	0.06	0.02
WP	0.00	0.76	0.90	-0.03	-0.24	0.18	0.00	0.78
				summer, 2 -month				
EA	-0.01	0.73	0.94	0.04	-0.17	0.24	0.00	0.74
EU	0.01	0.68	0.86	0.17	-0.04	0.37	0.03	0.10
NAO	0.00	0.76	0.91	0.03	-0.19	0.23	0.00	0.86
PNA	0.00	0.70	0.88	0.02	-0.19	0.23	0.00	0.86
WA	0.00	0.70	0.89	0.14	-0.07	0.34	0.02	0.20
WP	0.01	0.84	1.03	-0.16	-0.35	0.05	0.02	0.14
				summer, season				
EA	-0.01	0.59	0.76	0.32	0.12	0.49	0.10	0.00
EU	0.00	0.59	0.72	0.40	0.28	0.21	0.16	0.02
NAO	0.00	0.71	0.86	0.20	0.23	0.18	0.04	0.03
PNA	-0.01	0.55	0.71	0.26	0.26	0.06	0.14	0.01
WA	0.00	0.71	0.86	0.18	-0.03	0.38	0.03	0.08
WP	0.00	0.68	0.85	0.05	-0.16	0.26	0.00	0.63

Verification characteristics of 1- month, 2-month and 1-season lead forecast of 6 indices (ME is average, MAE is mean absolute and RMSE is mean square error, CC is correlation coefficient, CC1 and CC2 are lower and upper limits of confidence intervals CC, DT is the coefficient of determination, pval is the probability of error when the null hypothesis rejects for consistency with the available sample data for the summer period.

OPERATIONAL WORK

http://seakc.meteoinfo.ru

WMO | North Eurasia Climate Centre

Composite anomaly charts
(NCEP/NCAR, Reanalysis -2, means: 1981-2010)

Indices	Season	Parameter
EU	Summer	T at a height of 2 m

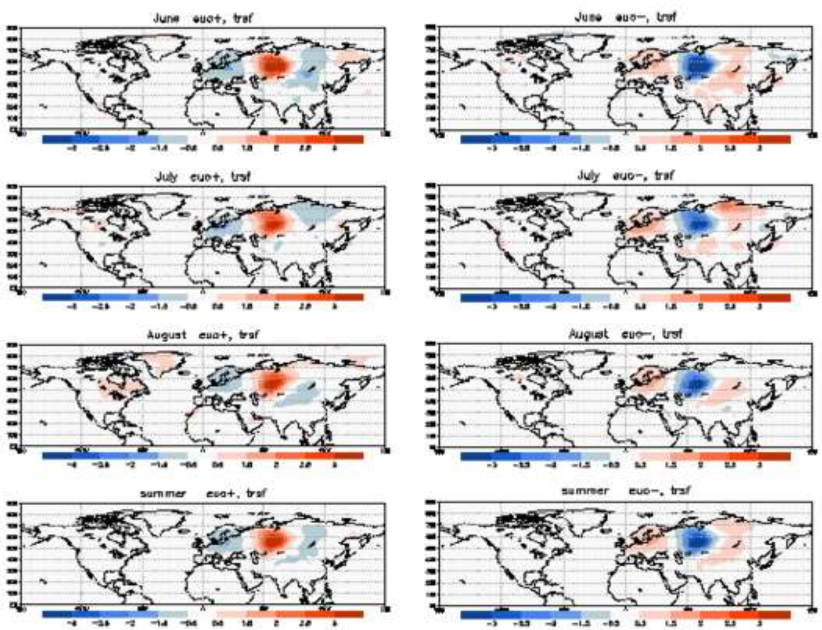

Figs. (left) and figs. (right) are the composites of the meteorological fields for the positive and negative phase of index respectively

White areas are not significant at 99% level of confidence.

The Model of Hydrometeorological centre of Russia Forecast

index	MAY, JUNE, JULY, AUGUST 2019					
	1 month	2 month	3 month	4 month	1 season	2 season
EA	-1,61	-1,45	-0,83	-0,44	-1,99	-1,03
WA	-1,29	-1,2	-2,32	-1,84	-1,63	-1,9
EU	-0,1	-0,06	0,08	-0,6	-0,07	-0,28
WP	0,49	-1,65	-0,66	0,36	-0,49	-0,79
PNA	0,38	0,84	-0,56	-0,06	0,63	0,11
NAO	-0,14	1,48	0,69	1,03	0,5	1,44
POL	0,14	-0,69	0,09	-0,52	-0,26	-0,33
AOS	0,36	0,1	0,1	-0,01	0,18	0,06

Red (blue) represents the positive (negative) phase of index

Designation

1. **EA** - East Atlantic Oscillation
2. **WA** - West Atlantic Oscillation
3. **EU** - Eurasia Pattern
4. **WP** - West Pacific Oscillation
5. **PNA** - Pacific – North American Pattern
6. **NAO** - North Atlantic Oscillation
7. **POL** - Polar Oscillation
8. **AOS** - Arctic Oscillation

Quartile Analysis of Indices

Index	Q1 (25%)	Q3 (75%)
EA	-0.493	0.485
WA	-0.559	0.494
EU	-0.452	0.458
WP	-0.544	0.501
PNA	-0.386	0.404
NAO	-0.487	0.632
POL	-0.487	0.632
AOS	-0.884	0.87

OPERATIONAL WORK

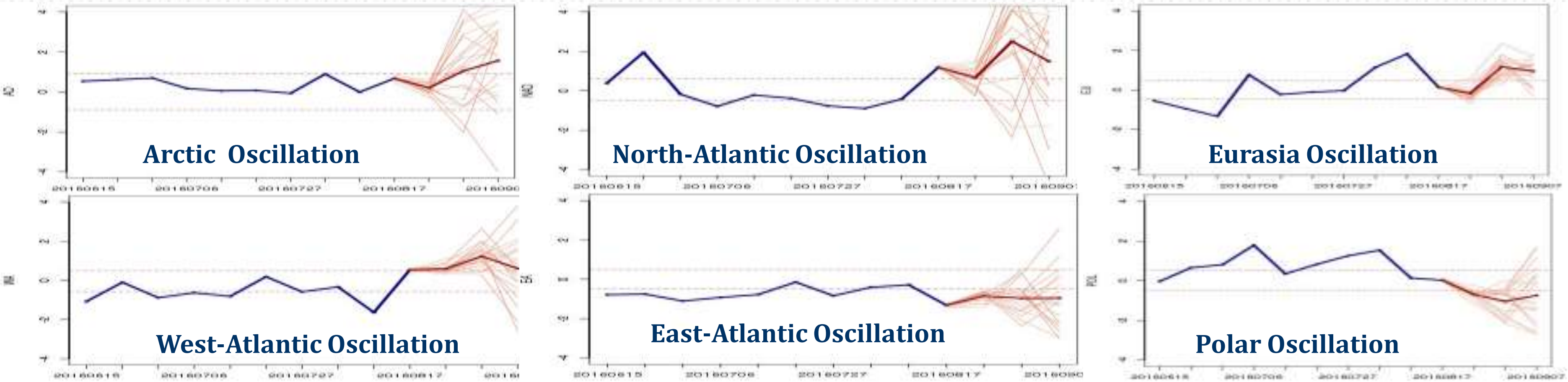

Intraseasonal (at weekly time intervals) variability of atmospheric circulation indices: observed (reanalysis, blue), predicted (red)

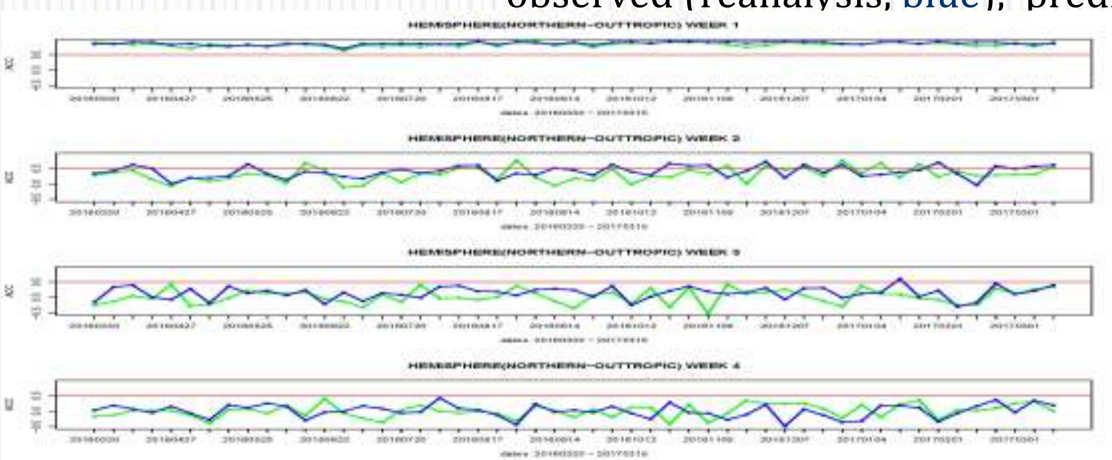

The first week

The second week

The third week

The forth week :

Atmospheric circulation forecasts: 500 hPa Anomalies, anomaly correlation coefficient (ACC) from March 30, 2016 to March 15, 2017 (51 cases).

Northern Hemisphere:
Forecasts of MGO (in blue), Forecasts of HMC (in green).

EXTREME EVENTS

(long-range forecasting)

- In recent years, significant progress has been made in the area of long-range meteorological forecasts (DMP). Despite the fact that the main products of Global Producing Centers of Long-Range Forecasts (GPCLRFs) WMO are forecasts of anomalies and / or probabilities of above, below or close to normal categories (for month, season), there are real possibilities for issuing forecasts of characteristics of extreme events. The main basis for the realization of such capabilities are Ensemble Prediction Systems (EPS). In the GPCLRFs sizes of ensembles are close to hundreds of forecast members, allowing us to construct various characteristics of extreme events.
- The easiest way is associated with the use of extreme averages for the period of forecast. Such forecasts are issued, for example, by the ECMWF, the Asia-Pacific Climate Center (APCC), the International Institute for Climate and Society (IRI), the French Meteorological Service (Meteo-France). Probabilities of “extreme” below (lowest ~15-20% of distribution) and above (highest ~15-20% of distribution) are predicted.
- The other way is connected with using the climatic indices (extreme values of daily mean, maximum and minimum temperature, heat and cold waves, circulation indices, etc.) on intra seasonal time scales.

EXTREME EVENTS

JUNE 2018

TEMPERATURE

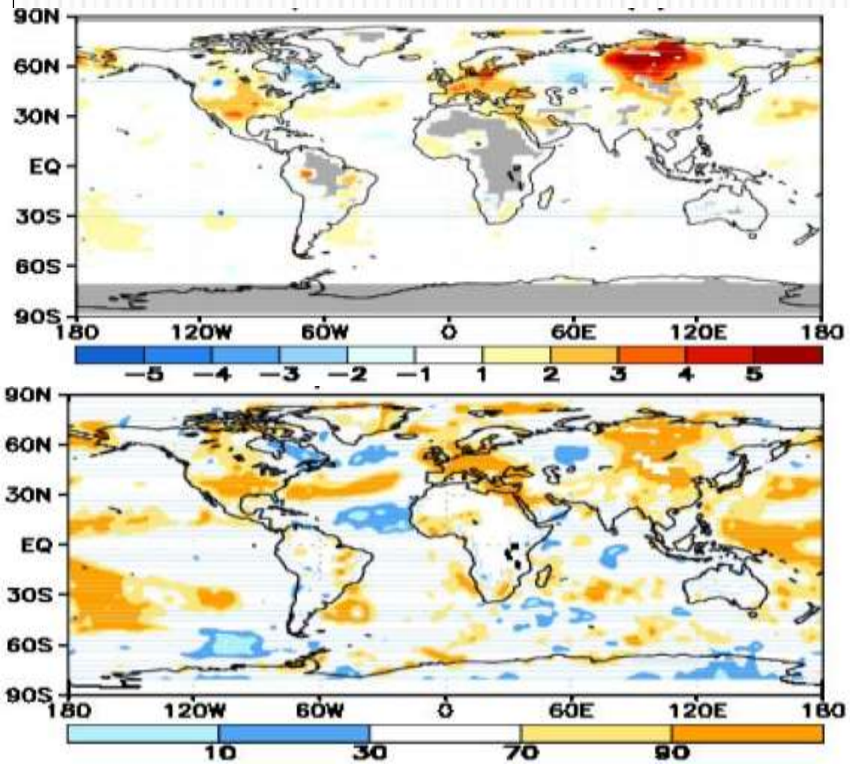

Surface temperature anomalies (°C, top) and surface temperature expressed as percentiles of the normal (Gaussian) distribution fit to the 1981-2010 base period (bottom). Analysis is based on station data over land and on SST data over the oceans (top).

PRECIPITATION

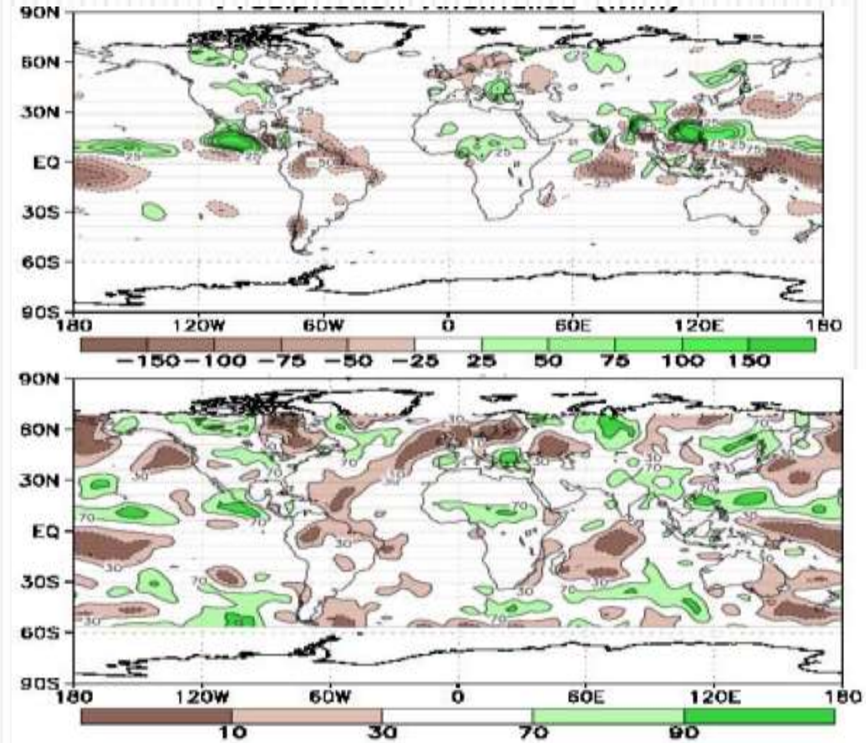

Anomalous precipitation (mm,top) and precipitation percentiles based on a Gamma distribution fit to the 1981-2010 base period (bottom). Data are obtained from a merge of raingauge observations and satellite – derived precipitation estimates. Contours are drawn at 200,100, 50,25,-25,-50,-100 and -200 mm in top panel. Percentiles are not plotted in regions where mean monthly precipitation < 5 mm/month.

CLIMATE DIAGNOSTIC BULLETIN,
Climate Prediction Centre,CPC

http://www.cpc.ncep.noaa.gov/products/CDB/CDB_Archive_pdf/pdf_CDB_archive.shtml

EXTREME EVENTS

JULY 2018

TEMPERATURE

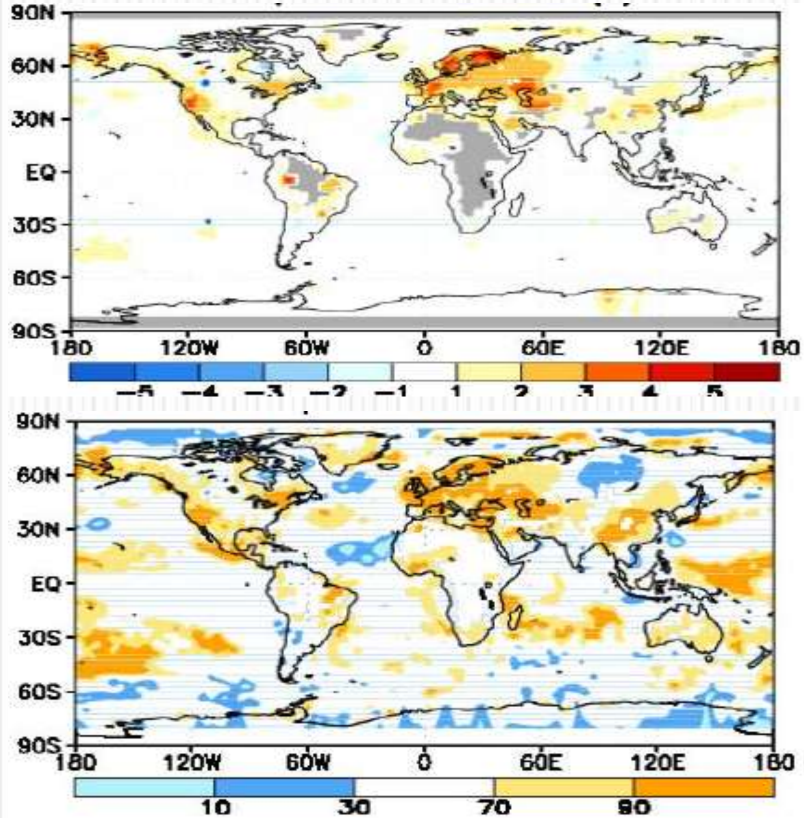

Surface temperature anomalies (°C, top) and surface temperature expressed as percentiles of the normal (Gaussian) distribution fit to the 1981-2010 base period (bottom). Analysis is based on station data over land and on SST data over the oceans (top).

PRECIPITATION

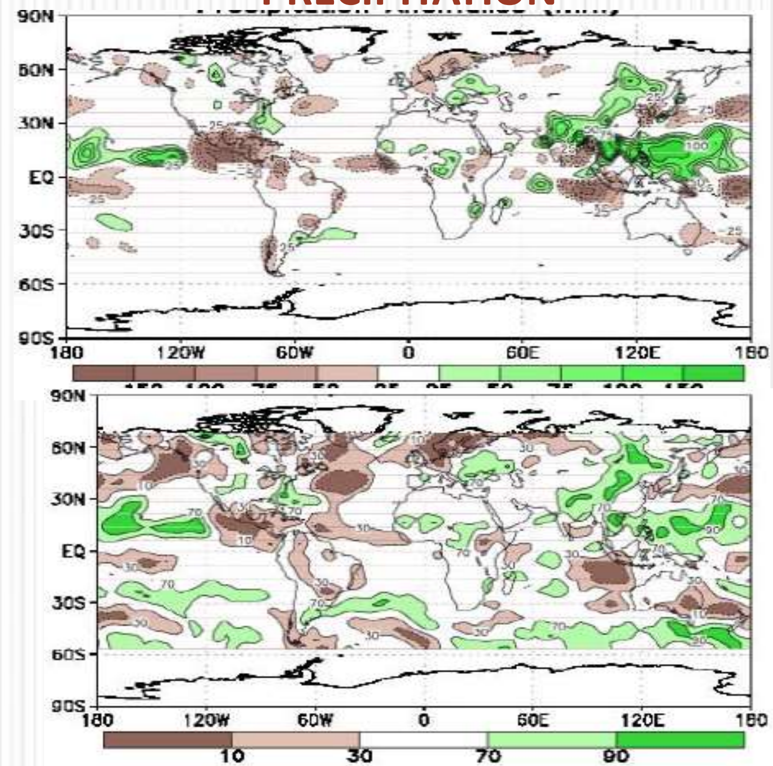

Anomalous precipitation (mm,top) and precipitation percentiles based on a Gamma distribution fit to the 1981-2010 base period (bottom). Data are obtained from a merge of raingauge observations and satellite – derived precipitation estimates. Contours are drown at 200,100, 50,25,-25,-50,-100 and -200 mm in top panel. Percentiles are not plotted in regions where mean monthly precipitation < 5 mm/month.

CLIMATE DIAGNOSTIC BULLETIN,
Climate Prediction Centre,CPC

http://www.cpc.ncep.noaa.gov/products/CDB/CDB_Archive_pdf/pdf_CDB_archive.shtml

EXTREME EVENTS

AUGUST 2018

TEMPERATURE

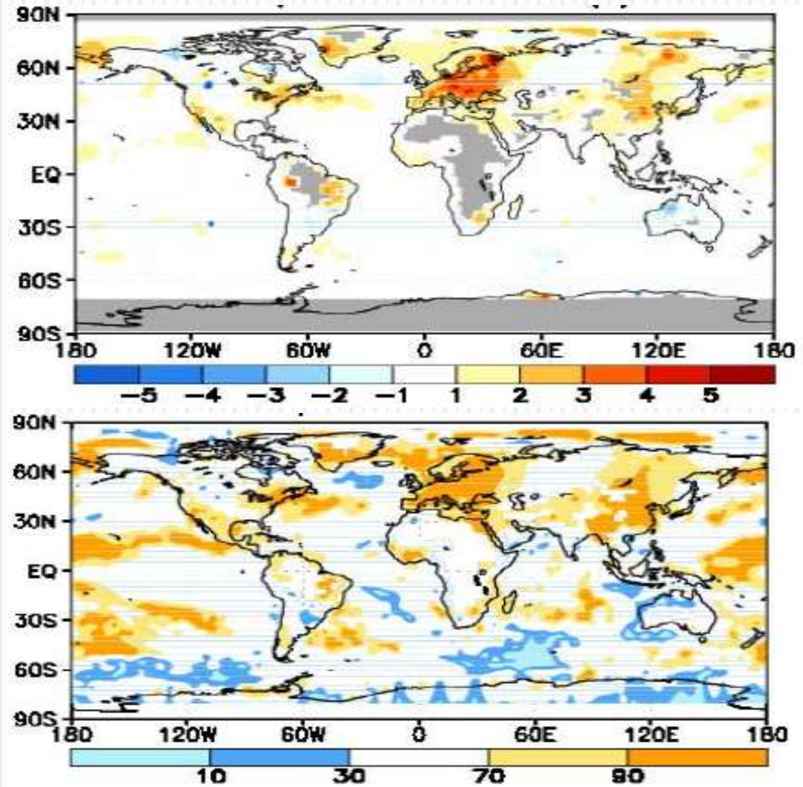

Surface temperature anomalies (°C, top) and surface temperature expressed as percentiles of the normal (Gaussian) distribution fit to the 1981-2010 base period (bottom). Analysis is based on station data over land and on SST data over the oceans (top).

PRECIPITATION

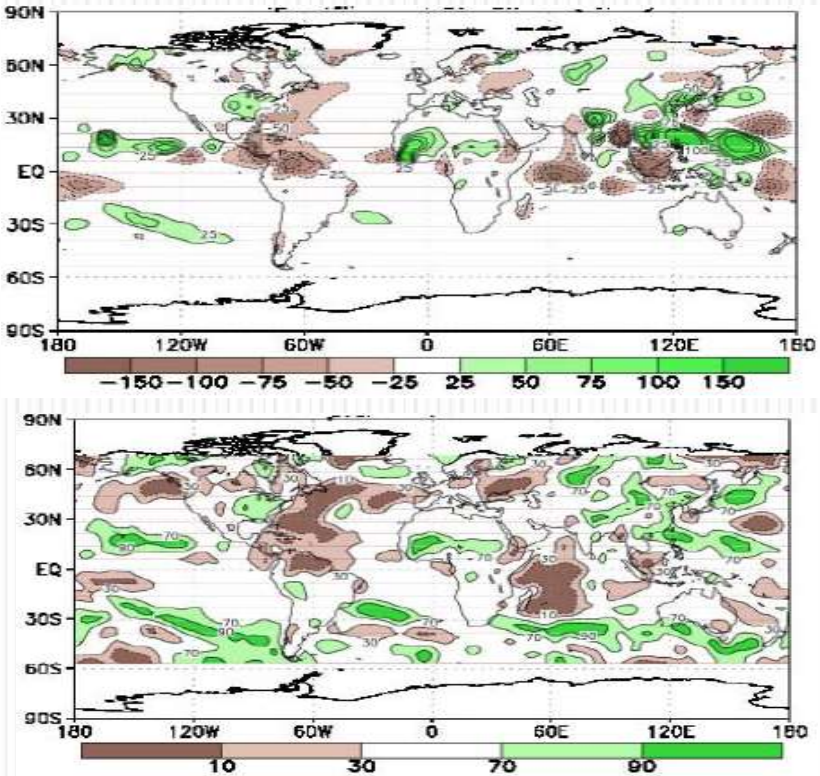

Anomalous precipitation (mm,top) and precipitation percentiles based on a Gamma distribution fit to the 1981-2010 base period (bottom). Data are obtained from a merge of raingauge observations and satellite – derived precipitation estimates. Contours are drown at 200,100, 50,25,-25,-50,-100 and -200 mm in top panel. Percentiles are not plotted in regions where mean monthly precipitation < 5 mm/month.

CLIMATE DIAGNOSTIC BULLETIN,
Climate Prediction Centre,CPC

http://www.cpc.ncep.noaa.gov/products/CDB/CDB_Archive_pdf/pdf_CDB_archive.shtml

EXTREME EVENTS

In Scandinavia, the temperature often exceeded the 30°C, and the monthly mean anomalies in some places were more than 5 ° C. In Sweden, the strongest fires in recent decades were raging.

A strong positive NAO pattern has been present for nearly all of 2018.

INDEX	MAY	JUNE	JULY	AUGUST	SEPTEMBER
NAO	2,0	1,4	1,4	2,4	1,8

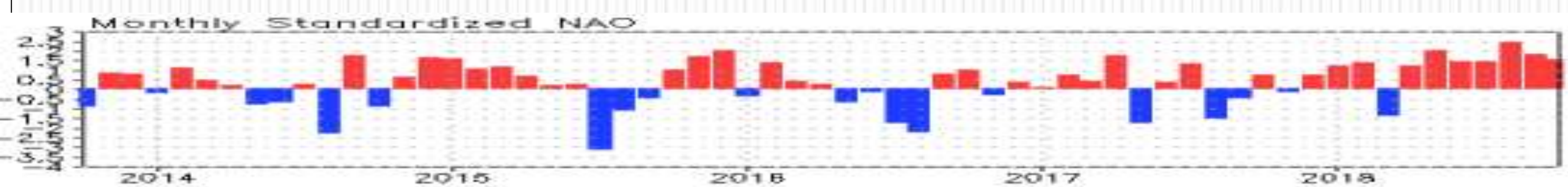

http://www.cpc.ncep.noaa.gov/products/CDB/CDB_Archive_pdf/pdf_CDB_archive.shtml

EXTREME EVENTS

SEA SURFACE TEMPERATURE

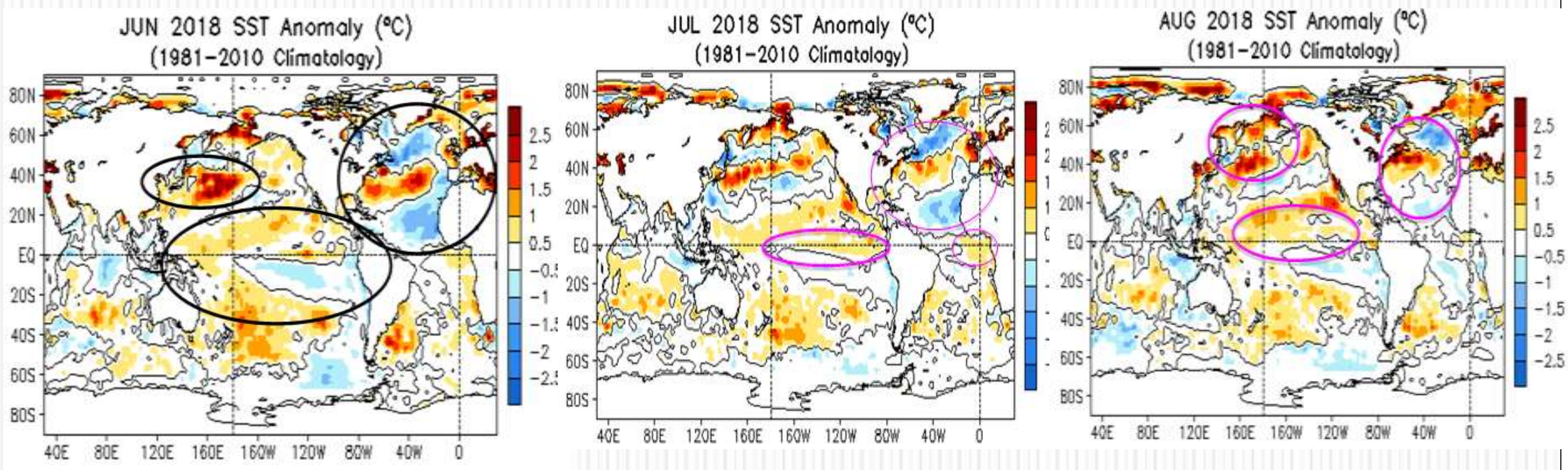

CLIMATE PREDICTION CENTRE

http://www.cpc.ncep.noaa.gov/products/CDB/CDB_Archive_pdf/pdf_CDB_archive.shtml

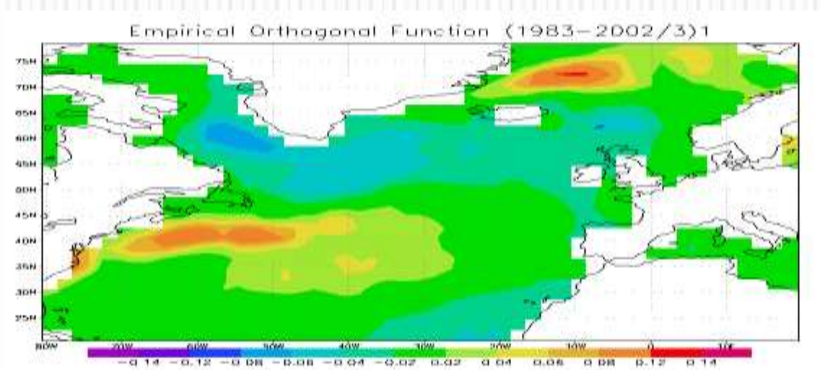

SST: First Empirical Orthogonal Function

North Atlantic: The tripole is the principal mode of SST variability in the North Atlantic (see picture). It was characterized by negative anomalies in the central part of the area .There were significant positive SST anomalies in the Gulf Stream and the NEO. Increasing temperature contrasts can lead to an exacerbation of atmospheric fronts and increased cyclonic activity . This means that the zonal transport of air mass is more intensive than it is necessary under the climate.

EXTREME EVENTS

FORECASTS AND OBSERVATIONS

July-August 2018

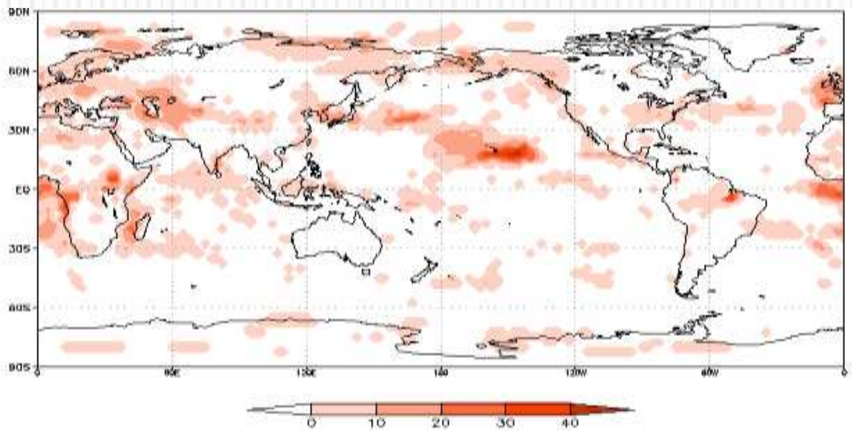

Predicted heat waves (45 days lead forecast)

Initial date: 05.07. 2018

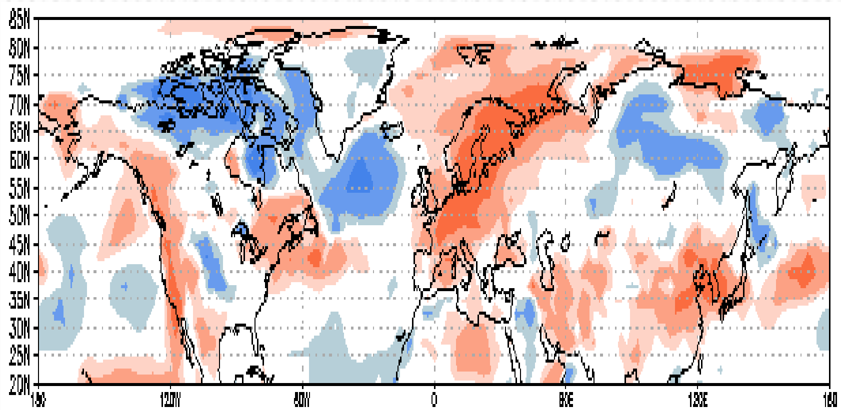

Observed, ERA, Interim: 45-daily mean

Extremes on the background of intraseasonal variability are identified using different climatic indices (for example, heat and cold waves).
WSDI index (heat waves): the number of days when at least for 5 consecutive days the temperature is> 90th percentile.
The Hydrometeorological Center of Russia has developed a technology of predicting heat and cold waves, as well as extreme forecast indices.
Data: the predicted fields of mean daily air temperature based on the ECMWF model, participated in the international S2S project (Subseasonal to Seasonal Prediction Project, http://s2sprediction.net/)
Heat waves in Europe and their propagation to the east, obtained on the basis of the ECMWF model, are in good agreement with the observed data.

EXTREME EVENTS

June 2018

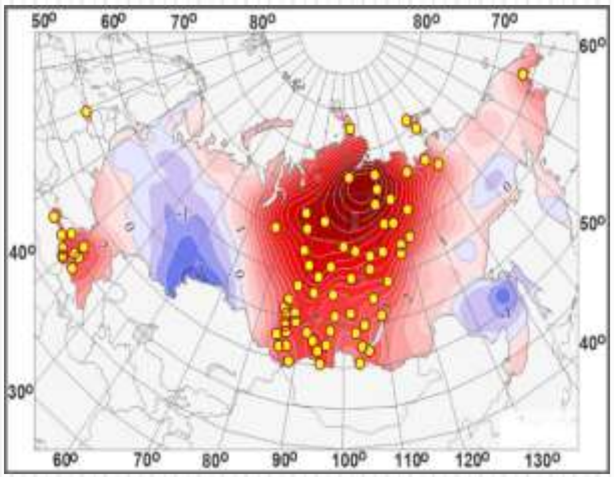

July 2018

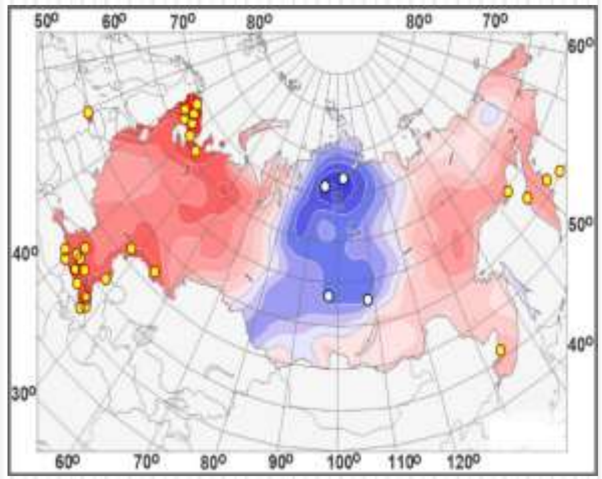

August 2018

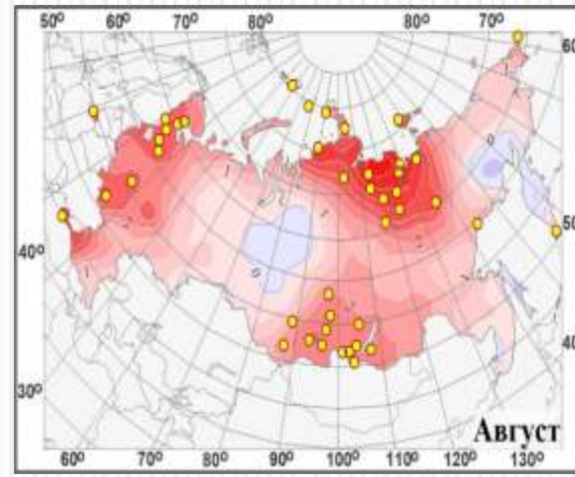

The white circles indicate the location of the station extremes below the 5th percentile, yellow - above the 95th percentile. Anomalies are calculated as deviations from the average for the base period 1961-1990. (IGCE)

INDEX	JUNE	JULY	AUGUST	SEPTEMBER	OCTOBER
SCAND	-0,77	2.27	-1.05	-0.74	-1,11

CLIMATE PREDICTION CENTRE

http://www.cpc.ncep.noaa.gov/products/CDB/CDB_Archive_pdf/pdf_CDB_archive.shtml

FORECASTS AND OBSERVATIONS

June – August 2018
2 m Temperature

Predicted GPC_Moscow

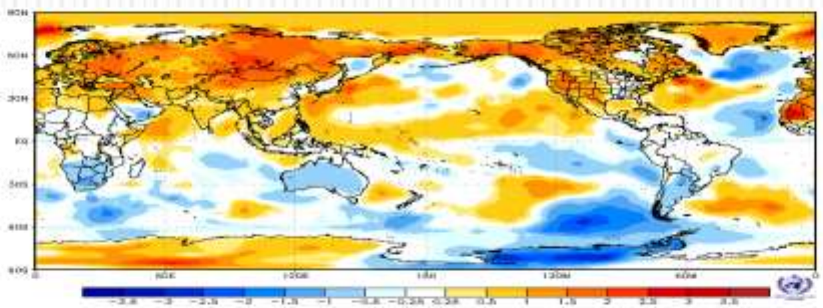

Observed (norm 1961-1990)

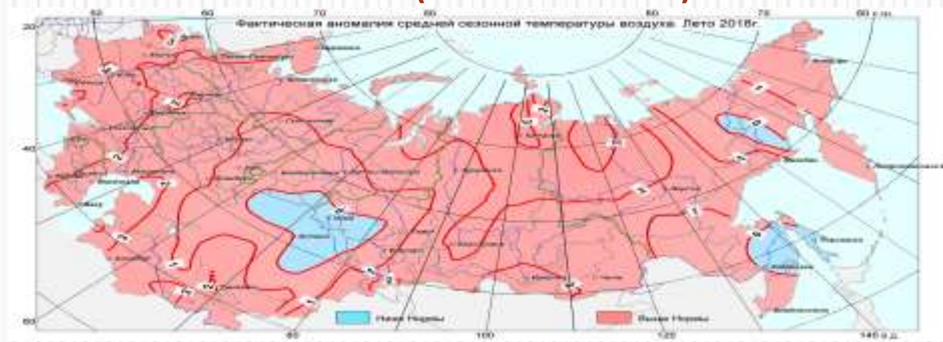

Predicted : LC MMELRF-WMO Lead Centre for MME LRF

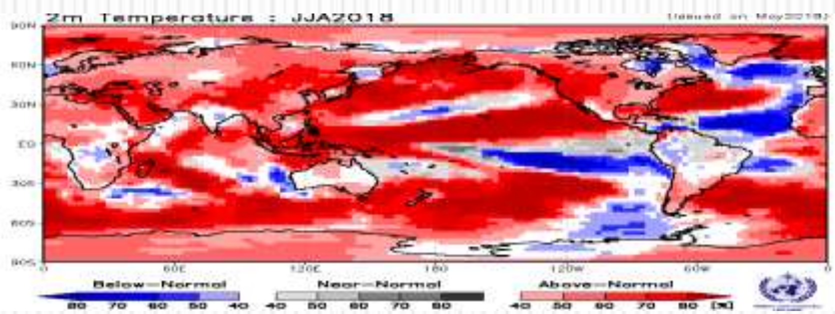

- **Temperature**: The summer of 2018 was warmer than normal over most of Northern Eurasia. The most significant anomalies (up to 2-3 degrees) were observed in the north of Eastern Siberia and northwest Yakutia. And only in the south of Western Siberia and northeastern Kazakhstan, the season was slightly cooler than usual.

Predicted: NEACC

Predicted: TOKYO CLIMATE CENTRE

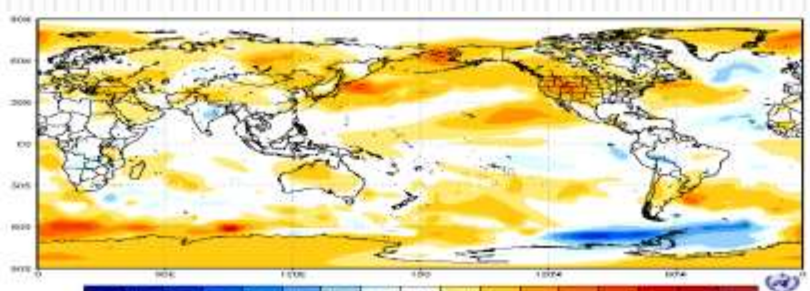

- **Comparison** of forecasts is made in a visual way. Positive temperature anomalies were predicted by many models. Weak negative anomalies were predicted only by TCC.

http://neacc.meteoinfo.ru

FORECASTS AND OBSERVATIONS

June – August 2018

Precipitation

Predicted: GPC_Moscow

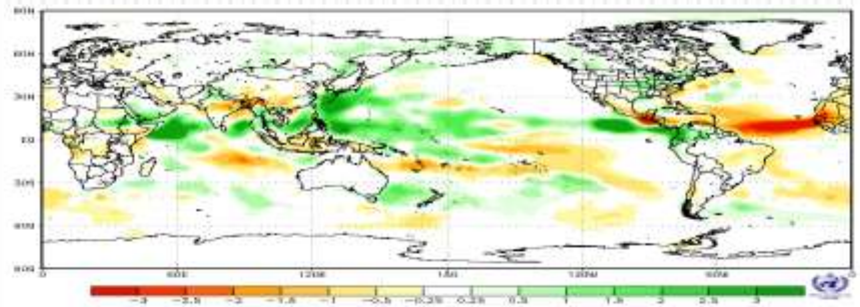

Predicted: LC MMELRF-WMO Lead Centre for MME LRF

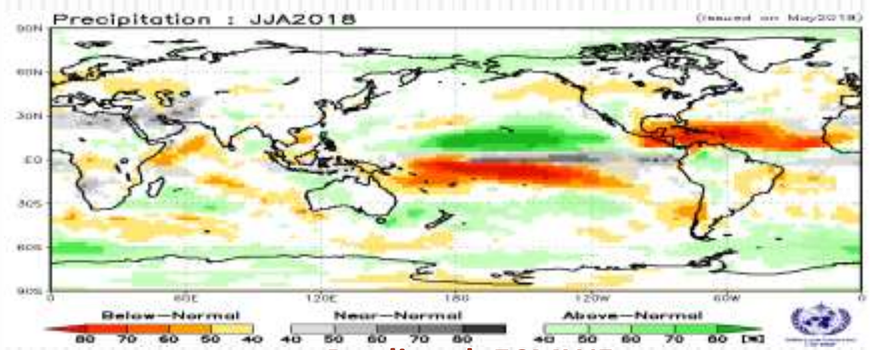

Predicted: ECMWF

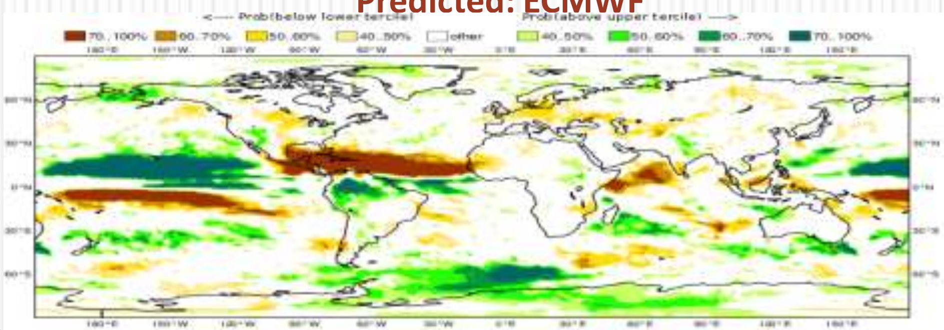

Observed (% from norm:1961-1990)

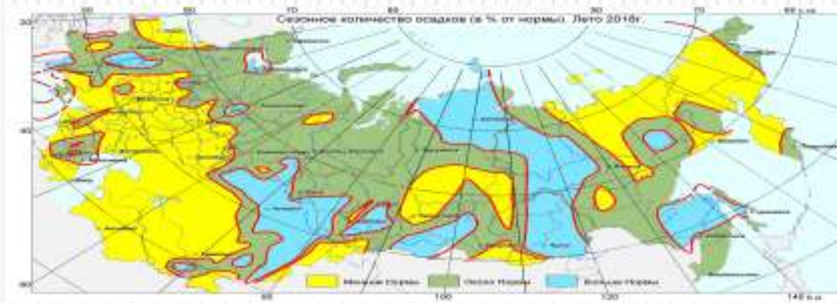

- **Precipitation:** Precipitation: there was a deficit of precipitation in the south of the European territory, over most of the Central Asia (except the northeast), as well as in the northeast of the Far East. There was an exceeding precipitation in the north-east of Kazakhstan, west of Yakutia, south of the Khabarovsk Cray.

Predicted: NEACC

Отрицательные аномалии осадков на юго-западе были предсказаны многими моделями.

http://neacc.meteoinfo.ru

SUMMARY

- The presented results are implemented in the work of long-rang forecast activities at the Hydrometeorological Research Centre of Russia (including NEACC). The forecasts of indices characterizing large-scale variability are operationally presented on the NEACC web-site and can be used by long-range forecasts experts, as well as when chart plotting of consensus forecasts at the climate forums.
- The use of the results is limited to forecasts of surface air temperature over most of regions. There are a lot of contradictions and uncertainties in the forecasts of precipitation. But knowledge about the strengthening or weakening of regional quasi-stationary waves associated with different phases of circulation indices may serve as an indirect sign of precipitation or, conversely, lack of precipitation.
- The quality of long-term forecasts varies greatly depending on the region, season, and atmospheric circulation regime. In this regard, promptly, forecasts of various indices can be used for an a priori estimation of the quality of forecasts.
- Analysis of large-scale atmospheric processes using teleconnection indices may be useful in studying the conditions of drought, flooding and other extreme climate events.

THANK YOU FOR ATTENTION!